Faking Giants: The Evolution of High Prey Clearance Rates in Jellyfishes

José Luis Acuña,[1]* Ángel López-Urrutia,[2] Sean Colin[3]

Jellyfishes have functionally replaced several overexploited commercial stocks of planktivorous fishes. This is paradoxical, because they use a primitive prey capture mechanism requiring direct contact with the prey, whereas fishes use more efficient visual detection. We have compiled published data to show that, in spite of their primitive life-style, jellyfishes exhibit similar instantaneous prey clearance and respiration rates as their fish competitors and similar potential for growth and reproduction. To achieve this production, they have evolved large, water-laden bodies that increase prey contact rates. Although larger bodies are less efficient for swimming, optimization analysis reveals that large collectors are advantageous if they move through the water sufficiently slowly.

Several trophic systems have shifted from being planktivorous fish-dominated to jellyfish-dominated after overfishing (*1*–*5*), hinting at a future "gelatinous" ocean reminiscent of the early Ediacaran if fishing effort and other anthropogenic stressors remain unchanged (*6*). Indeed, growing evidence of dietary, spatial, and temporal overlap among planktivorous fishes and jellyfishes (*7*–*9*) points to some degree of competition (*10*, *11*). High fishing pressure on fish would favor a shift toward the competitively inferior jellyfishes (*11*). Contrasting competitive abilities between fishes and jellyfishes have been attributed to feeding differences among visual and tactile predators (*12*). Most economically relevant fishes and trophically dominant jellyfishes are cruising predators, which hunt while swimming. Fishes have compact bodies and use their eyes to detect prey. In contrast, swimming medusae pulse their bells to create vortices that serve as a feeding current and transport prey to their tentacles and oral arms (Fig. 1). Compared with fishes of the same length, jellyfishes exhibit lower clearance rates, that is, volume of water cleared of prey per unit time (*12*). However, jellyfishes are watery animals, containing less than 1.5 kg of carbon per cubic meter of body volume, as opposed to 100 kg of C m^{-3} in organisms with a normal carbon content (*13*). Thus body carbon, rather than length, may be the relevant metric when comparing physiological rates among organisms (*14*). Further, the competitive ability of a predator depends not only on prey capture and ingestion rates but on how efficiently the energy obtained translates into body growth and population buildup. This requires an analysis of the energy balance, involving not only the feeding benefits but also the respiratory losses. The difference between these two is the scope for growth, which can be defined as

$$H = G - R = lCPe - R \quad (1)$$

where G is the energy input from food assimilation, R is the total respiration rate, l is the proportion of day spent feeding, C is the clearance rate, P is the prey density, and e is the digestive assimilation efficiency. The scope for growth indicates the potential for growth and is related to the rate of biomass and population buildup; thus, it is an indicator of competitive performance.

We have compiled published data on clearance (table S1) and respiration rates (table S2) of fishes, jellyfishes, and their crustacean prey to compare their bioenergetic performance in marine food webs (*15*) (Fig. 2). In a log-log plot, the allometric regressions of clearance rate versus body carbon for jellyfishes ($n = 364$) and for fishes ($n = 243$) were nearly identical (Fig. 2A), with similar slopes [general linear model, test for heterogeneity of slopes, $t_s = 0.091$, $P = 0.928$, table S3 (*15*)] and intercepts (general linear model, test for heterogeneity of intercepts, $t_i = 1.962$, $P = 0.050$; table S3), and a regression model with common slope and intercept was the most parsimonious [i.e., it scored the lowest in the Bayesian information criterion (BIC), table S3]. In contrast, the crustacean ($n = 667$) and jellyfishes lines had different slopes ($t_s = -5.152$, $P < 0.001$) and differed significantly within the full range of body carbon overlap, being best described by a model with separate regressions (table S3). In contrast, all three groups clustered together in a respiration versus body carbon log-log plot (Fig. 2C). The jellyfishes line ($n = 567$) and the line formed by pooling the fishes ($n = 243$) and the crustaceans ($n = 1421$) data shared similar slopes ($t_s = 1.936$, $P = 0.053$) and intercepts ($t_i = 1.935$, $P = 0.053$), being best described by a model with common slope and intercept (table S3). This confirms that organisms with the same body carbon respire similarly (*14*). Thus, jellyfishes and fishes capture and consume prey at similar rates with similar respiration costs and scope for growth, suggesting the absence of a major disadvantage in terms of prey capture mechanism (*12*). Because of their higher clearance rates, they should cease to grow at lower prey concentrations than crustaceans. This is best evaluated by the threshold prey concentration, $P_{H=0}$, where feeding benefits equal respiration losses. $P_{H=0}$ can be found by setting $H = 0$ in Eq. 1 and solving for P to arrive at $P_{H=0} = R/lCe$. We can combine this equation with reasonable figures for l, R, C, and e (table S5) to estimate $P_{H=0}$. Accordingly, jellyfishes, fishes, and crustaceans of average body carbon (0.0036, 0.068, and 0.00014 g of C per individual, respectively; geometric mean calculated with individuals used for respiration and clearance data; tables S1 and S2) would starve (negative scope for growth) below threshold prey concentrations $P_{H=0}$ of 14, 14, and 168 μg of C l^{-1}, respectively. These figures may be brought down by an order of magnitude by assuming that the organisms increase their clearance rates in response to lowered food concentrations or optimal prey sizes [supporting online material (SOM) text and table S5], but the pattern persists: Fishes and jellyfishes can thrive at lower prey concentrations than their crustacean prey.

In terms of fresh body weight, the situation is apparently inverted: The clearance line for jellyfishes leveled with the crustacean line (Fig. 2B). Their slopes were heterogeneous ($t_s = -3.855$, $P < 0.001$; same sample sizes as in the comparisons above), and a separate regressions model was favored by the BIC, although their lines differed only outside a log(wet weight, g) range from –5.23 to –0.78 (table S3). In contrast, the jellyfishes were well below the fishes line (Fig. 2C), their slopes were heterogeneous ($t_s = 3.434$; $P < 0.001$), their lines differed across the full range of wet body weights, and a separate regressions model scored the lowest BIC (table S3). This

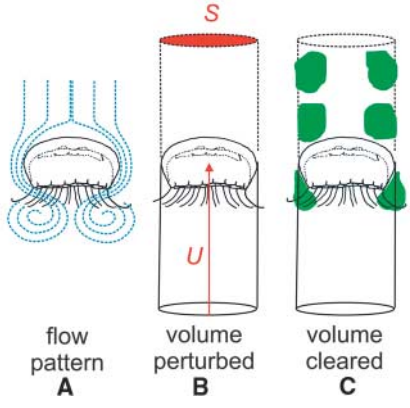

Fig. 1. Prey capture in cruising medusae. (**A**) Flow around a medusa during bell contraction (blue lines). Fluid is transported from in front of the medusae, along the bell margin, and into trailing vortices to circulate through the capture surfaces (i.e., tentacles). (**B**) The volume of fluid that they swim through can be approximated as a cylinder (in red) with dimensions determined by the projected surface area (*S*) of the medusae and its velocity (*U*). (**C**) However, only a portion of the cylinder of fluid (volume in green) actually interacts with the capture surfaces, determined by the part of the swimming cycle that the fluid passes by the medusan bell (*20*) [see figure 13 of (*21*)]. Although powered by ciliary movement, a similar process applies to ctenophores.

[1]Departamento de Biología de Organismos y Sistemas, Universidad de Oviedo, Calle Catedrático Rodrigo Uría, sin número, 33071 Oviedo, Spain. [2]Instituto Español de Oceanografía, Centro Oceanográfico de Gijón, Avenida Príncipe de Asturias, 70 bis, 33212 Gijón, Spain. [3]Department of Marine Biology and Environmental Sciences, Roger Williams University, Bristol, RI 02809, USA.

*To whom correspondence should be addressed. E-mail: acuna@uniovi.es

would seem to confirm the idea of a marked disadvantage because of the feeding mechanism of jellyfishes (*12*), but their lower clearance rates are compensated by an order of magnitude lower respiration rates (Fig. 2D). The slopes of the jellyfishes respiration line and that for pooled crustaceans and fishes were not heterogeneous ($t_s = 1.837$, $P = 0.066$), but the intercepts differed significantly ($t_i = 74.589$, $P < 0.001$), which is confirmed by the BIC (table S3). This suggests that, whereas fishes achieve high clearance rates through visual predation, jellyfishes rely on body augmentation. It also poses an interesting problem, because bearing eyes comes with little hydromechanical cost, whereas an inflated body is harder to move through the water. Jellyfishes have surmounted this problem by keeping swimming costs low. Log-log regressions of cruising velocity versus body size for jellyfishes ($n = 67$) had similar slopes and lower intercepts than those for crustaceans ($n = 37$; $t_s = 0.394$, $P = 0.694$ and $t_i = 3.298$, $P = 0.001$ for body carbon as covariate; $t_s = -0.646$, $P = 0.520$ and $t_i = 7.706$, $P < 0.001$ for wet weight as covariate; table S3), and, except for a set of observations in the cannonball jellyfish *Stomolophus meleagris*, all measurements of swimming velocity of jellyfish fell below the lower 95% confidence intervals for the fishes regressions ($n = 49$), both in terms of body carbon (Fig. 3A) and wet weight (Fig. 3B). Three other jellyfish species and one ctenophore for which neither body carbon nor wet weight were available were also slow cruisers, with velocities ranging from 0.4 to 3 cm s^{-1} (table S7). We next use cost-benefit optimization theory to analyze the nature of this adaptation.

To model the feeding benefits, we will assume that the total volume cleared from prey by a cruising predator is proportional to its swimming velocity, U, and to its projected cross surface, S (*16*, *17*), such that

$$C = \beta SU \quad (2)$$

where β is a searching efficiency corresponding to the ratio of volume actually cleared from prey (green in Fig. 1C) to volume perturbed (cylinder in Fig. 1B). Solving Eq. 2 we arrive at $\beta = C/SU$, which can be combined with estimates or measurements of C, S, and U to calculate β. This simple exercise reveals that the searching efficiency β ranges between 0.02 and 2.7 in jellyfishes, with a geometric mean at 0.089, whereas it varied between 3 and 5 within the estimation body size range in fishes (Fig. 3, C and D). In other words, the evolution of high clearance rates involves a tendency toward small S and large β in visual predators—that is, large search area relative to cross body surface—but the reverse in contact cruising predators.

In Ware's theoretical framework (*16*), the total respiration of a cruising predator integrates a fixed maintenance cost, R_b, plus a variable swimming cost, D. In jellyfish, the latter can be estimated from biomechanical equations for the drag of a hemispherical body moving through the water (*18*) such that

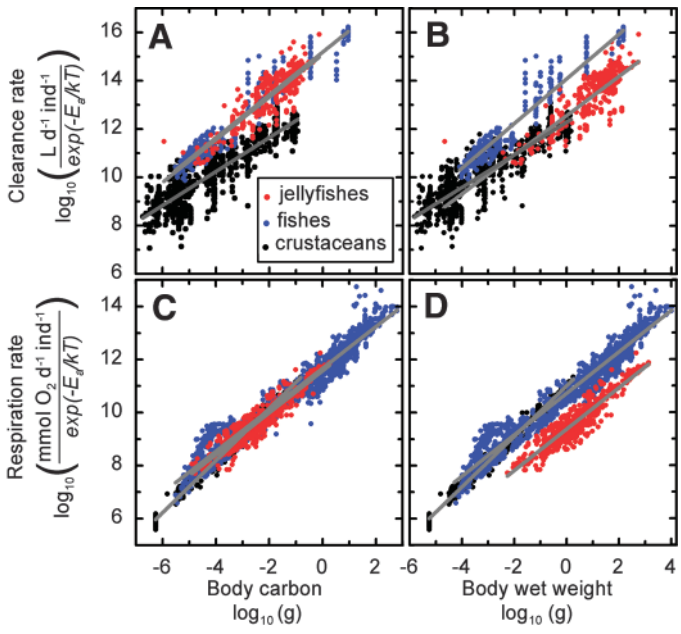

Fig. 2. Log-log plots of temperature-corrected clearance rates (**A** and **B**) and temperature-corrected respiration rates (**C** and **D**) versus body carbon (left) and body wet weight (right) for fish (blue), jellyfish (red), and their crustacean prey (black). E_a is the activation energy (assumed to be 0.65 eV), k is Boltzmann's constant (0.0000862 eV K^{-1}), and T is the absolute temperature (in K) (*15*).

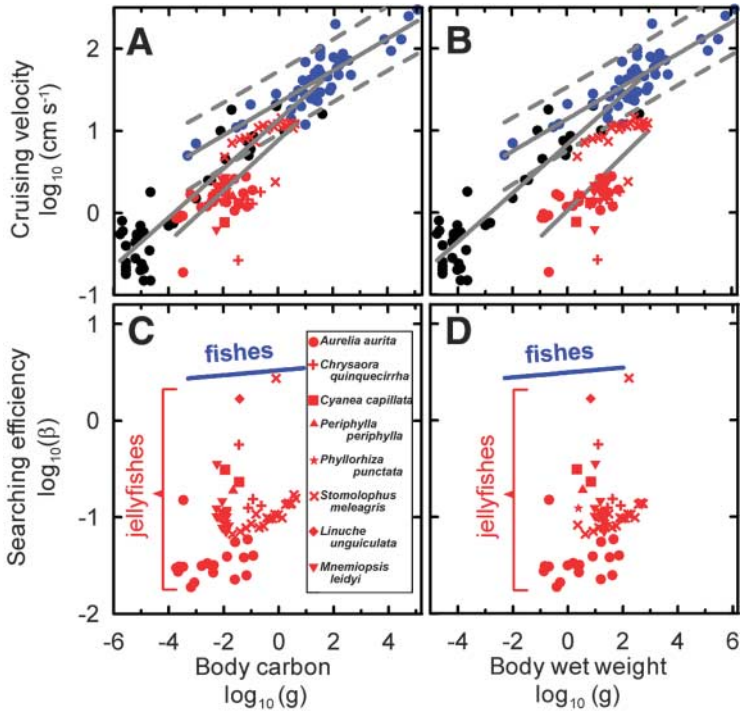

Fig. 3. (**A** and **B**) Log-log plots of cruising (not escape) velocity versus body carbon (A) and body wet weight (B). Data for fish (blue) and crustaceans (black) are from (*22*), after assuming a body carbon–to–volume conversion of 100 kg of C m^{-3} from (*13*) and the same density as seawater. Data for jellyfishes [different symbols for each species, with meanings in (C)] are from our data compilation in table S7. Thick gray lines indicate ordinary least squares log-log fits for each group (comparison among lines and regression statistics in tables S3 and S4, respectively). Dashed gray lines correspond to the 95% confidence intervals for individual predictions for the fish regression. (**C** and **D**) Estimated searching efficiencies versus body carbon and body wet weight for fishes (blue line) and jellyfishes (red symbols). The fish line was estimated by rearranging Eq. 2 as $\beta = C/SU$ and combining this equation with values of C and U estimated from allometric equations in Figs. 2A and 3A (table S4) and values of S estimated by assuming cylindrical shape and an approximate width:length ratio of 7:1, as in (*22*). For jellyfishes, we combined each pair of observed U and S (Fig. 3A and table S7) with an estimate of C according to the allometric equation in Fig. 2A (table S4), arriving at a single estimate of β for every cruising velocity measurement.

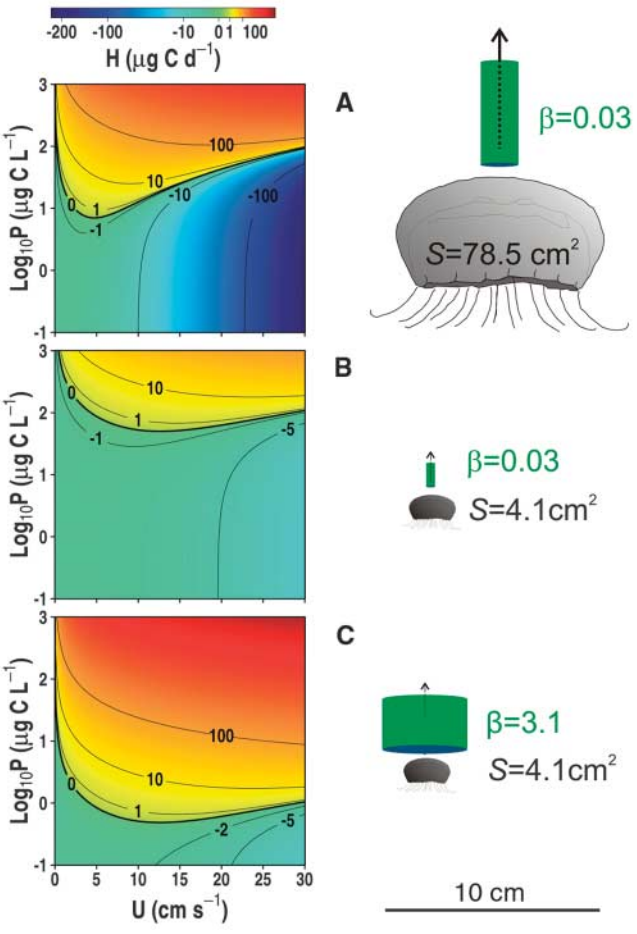

Fig. 4. Plot of the scope for growth, *H*, versus the prey concentration, *P*, and the swimming velocity, *U*, according to Eq. 4, for (**A**) a 10-cm-diameter *A. aurita*, (**B**) a hypothetical nongelatinous *A. aurita* with the same carbon content as that in (A) but a correspondingly smaller collector surface *S*, and (**C**) same as in (B) but assuming the searching efficiency β of a fish with similar body carbon, according to the line in Fig. 3, C and D. Sources, parameter values, calculations, and assumptions are in table S8. Colors indicate values of *H*, with green to red for positive and blue for negative growth rates. Thin lines indicate logarithmically distributed growth isolines. The thick line corresponds to the 0-growth isocline, $P_{H=0}$.

$$R = D + R_b = \frac{1}{2\eta}\alpha C_D \rho S U^3 + R_b \qquad (3)$$

where η is the propulsive efficiency, ρ is the water density, and C_D is the drag coefficient. We can now substitute *C* and *R* in Eq. 1 by the right-hand sides of Eqs. 2 and 3, respectively, and, assuming that $l = 1$ for jellyfish (table S5), arrive at

$$H = \beta SUPe - \frac{1}{2\eta}\alpha C_D \rho S U^3 - R_b \qquad (4)$$

H represents the scope for growth of a jellyfish, taking into account feeding benefits, swimming costs, and basal metabolism. Figure 4A represents *H* against swimming velocity and prey concentration for a 10-cm moon jellyfish *Aurelia aurita*, assuming reasonable values for the parameters of Eq. 4 (table S8). The diagonal ridge crossing the function from lower left to upper right is due to the functional relationship with the swimming velocity, which is cubic in the case of *D* but only linear for the feeding benefits (Eq. 4). The scope for growth is positive above a threshold prey concentration $P_{H=0}$, which varies as a function of the swimming velocity. Because of the characteristic ridge in the *H* function, $P_{H=0}$ reaches a minimum for an optimal swimming velocity (Fig. 4A), which is found by setting $\frac{dP_{H=0}}{dU} = 0$ and solving for *U* (SOM text), yielding

$$U_{opt} = \left(\frac{\eta R_b}{\alpha C_D \rho S}\right)^{\frac{1}{3}} \qquad (5)$$

Equation 5 implies that the evolution of larger *S*, that is, larger bell surfaces and more gelatinous bodies to sustain them, will lead to slower cruising velocities. An *A. aurita* jellyfish 10 cm in diameter swims at $U = 2.2$ cm s^{-1}, in the vicinity of $U_{opt} = 4.7$ cm s^{-1} (Fig. 4A). Thus, it grows almost at the lowest possible prey concentration ($P_{H=0}$ at U_{opt} is 7 μg of C l^{-1}) and sustains only mild shrinking rates when starving, because of the moderate slope of the *H* function at U_{opt} (Fig. 4A), explaining their capacity to endure months of shrinkage when prey is scarce (*19*). By contrast, a hypothetical nongelatinous *A. aurita* with the same body carbon but a normal water content and a concomitantly smaller *S* would have an $U_{opt} = 12.7$ cm s^{-1} (Fig. 4B), switching to shrinkage at $P_{H=0} = 50$ μg of C l^{-1}, which suggests that being gelatinous allows access to lower prey concentrations. Note that U_{opt} is independent of β (Eq. 4); therefore, evolution of high β, the fish strategy, brings the minimum of the $P_{H=0}$ threshold function down to very low prey concentrations while preserving its blunt shape (Fig. 4C), rendering this strategy less sensitive to foraging velocity optimization.

It seems that jellyfish have responded to the selective pressure of prey dilution typical of life as predators by evolving large bodies and collection structures while keeping the dynamic component of the feeding process, the swimming velocity, slow. Unlike fish, being large and slow may render jellyfishes more vulnerable to predation and passively dependent on ocean currents for sex encounter and recruitment to benthos. However, our work suggests that their bioenergetic performance is very similar. By using their primitive feeding systems, jellyfishes achieve instantaneous production rates similar to those of fishes and are capable of capitalizing on ecosystem changes resulting from overfishing.

References and Notes

1. T. Kawasaki, *Fish. Oceanogr.* **2**, 244 (1993).
2. T. A. Shiganova, *Fish. Oceanogr.* **7**, 305 (1998).
3. C. P. Lynam *et al.*, *Curr. Biol.* **16**, R492 (2006).
4. G. M. Daskalov, A. N. Grishin, S. Rodionov, V. Mihneva, *Proc. Natl. Acad. Sci. U.S.A.* **104**, 10518 (2007).
5. R. D. Brodeur, H. Sugisaki, G. L. Hunt Jr., *Mar. Ecol. Prog. Ser.* **233**, 89 (2002).
6. T. R. Parson, C. M. Lalli, *Mer* **40**, 111 (2002).
7. J. E. Purcell, *Can. J. Fish. Aquat. Sci.* **47**, 505 (1990).
8. J. E. Purcell, M. V. Sturdevant, *Mar. Ecol. Prog. Ser.* **210**, 67 (2001).
9. R. D. Brodeur, C. L. Suchman, D. C. Reese, T. W. Miller, E. A. Daly, *Mar. Biol.* **154**, 649 (2008).
10. J. E. Purcell, S. Uye, W. T. Lo, *Mar. Ecol. Prog. Ser.* **350**, 153 (2007).
11. A. J. Richardson, A. Bakun, G. C. Hays, M. J. Gibbons, *Trends Ecol. Evol.* **24**, 312 (2009).
12. T. A. Sørnes, D. L. Aksnes, *Limnol. Oceanogr.* **49**, 69 (2004).
13. A. Vinogradov, *The Elementary Composition of Marine Organisms* (Yale Univ. Press, New Haven, CT, 1953).
14. G. Schneider, *Helgol. Mar. Res.* **46**, 377 (1992).
15. Materials and methods are available as supporting material on *Science* Online.
16. D. M. Ware, *J. Fish. Res. Board Can.* **35**, 220 (1978).
17. T. Kiørboe, *A Mechanistic Approach to Plankton Ecology* (Princeton Univ. Press, Princeton, NJ, 2008).
18. T. L. Daniel, *Can. J. Zool.* **61**, 1406 (1983).
19. M. N. Arai, A *Functional Biology of Scyphozoa* (Chapman and Hall, New York, 1997).
20. J. O. Dabiri, S. P. Colin, J. H. Costello, M. Gharib, *J. Exp. Biol.* **208**, 1257 (2005).
21. S. C. Shadden, J. O. Dabiri, J. E. Marsden, *Phys. Fluids* **18**, 047105 (2006).
22. M. E. Huntley, M. Zhou, *Mar. Ecol. Prog. Ser.* **273**, 65 (2004).

Acknowledgments: We thank A. Bochdansky for fish respiration data and F. González-Taboada for help with statistics. This research has been financed by project MALASPINA 2010 (MICINN-08-CSD2008-00077, Spanish Ministry of Science) to J.L.A. and A.L.-U., partially funded by a Campus of International Excellence grant from the Administration of the Principality of Asturias to the University of Oviedo, by Theme 6 of the European Commission Seventh Framework Programme through the Marine Ecosystem Evolution in a Changing Environment (MEECE No 212085) Collaborative Project to A.L.-U., and by awards from NSF to S.C. (OCE-0623534 and -0727544) and from the Office of Naval Research (N000140810654). The present data compilation is available in the form of tables in the SOM.

Supporting Online Material

www.sciencemag.org/cgi/content/full/333/6049/1627/DC1
Materials and Methods
SOM Text
Figs. S1 to S3
Tables S1 to S8
References (*23*–*106*)

3 March 2011; accepted 9 August 2011
10.1126/science.1205134